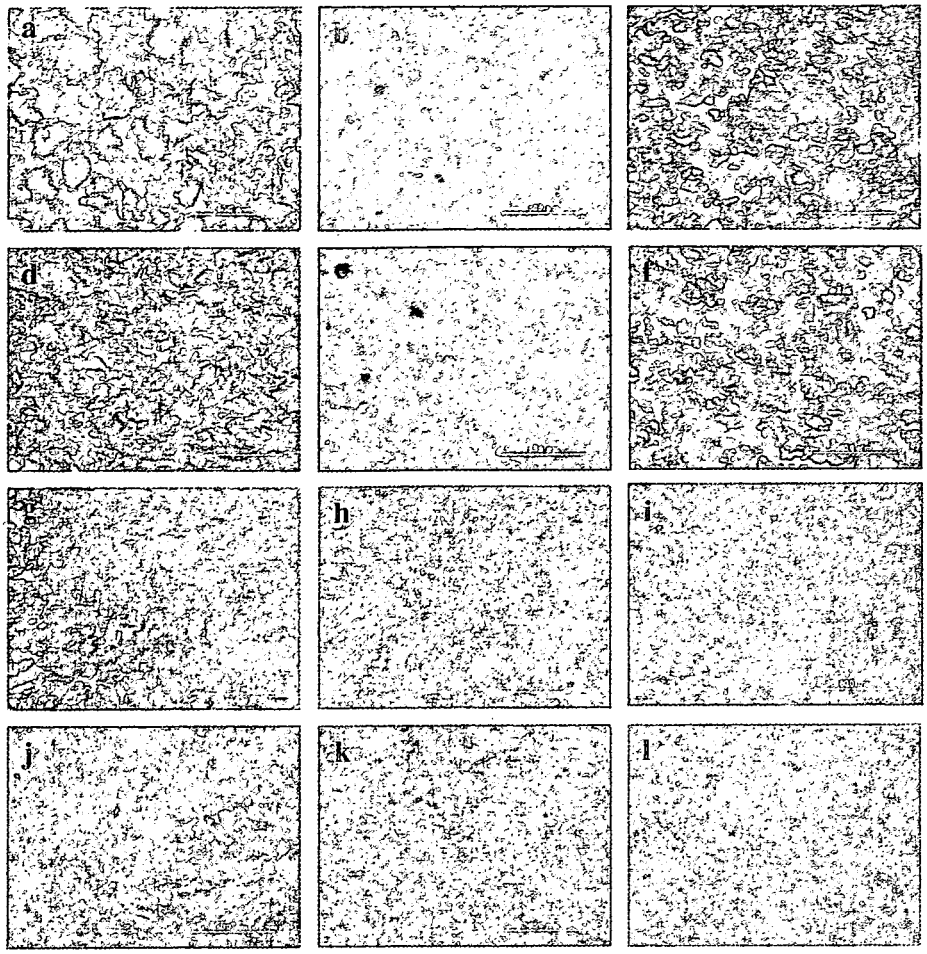

Fig. 6. Type I collagen (a, d, g, j), type II collagen (b, e, h, k), and cartilage proteoglycan (c, f, i, l) staining of pellets that formed on PAAm- (a–c), PEG- (d–f), PAAc-modified (g–i), and control (j–l) surfaces after culture in chondrogenic induction medium for 2 weeks. The scale bar is 50 μm.

demonstrated the early effects of chargeable polymer-modified surfaces on the chondrogenic differentiation of MSCs, and the results might be applicable to other chargeable polymers. Surfaces presenting methyl, hydroxyl, carboxyl, and amino groups have been reported to affect cell functions through modulating fibronectin structure and the availability of binding/receptor sites [24,25]. The different effects of the PAAm-, PEG-, PAAc-modified and control surfaces in the present study may be mediated by adsorbed proteins.

Curran et al. [15,16] reported that $-NH_2$ surfaces did not support chondrogenic differentiation of MSCs in serum medium, but did promote chondrogenesis when cultured in the chondrogenic differentiation medium. –COOH surfaces promote chondrogenesis in both serum medium and induction medium. In the present study, the effect of PAAc-modified surfaces is different from their results. The difference might result from different cell culture conditions. They used a monolayer culture to investigate the effects. However, in this study, at the first stage, the cells on the PAAm-, PAAc-modified, and control surfaces were monolayer and then formed pellets after a few days of culture. The pellets can provide a three-dimensional microenvironment that facilitates chondrogenic differentiation. When cultured on the surface of culture plate for a few passages, primary chondrocytes may change from their original round morphology to a spindle, fibroblast-like shape and lose their ability to express articular cartilage-specific ECMs such as type II collagen and aggrecan. Instead, they express and produce fibroblast-specific ECM, type I collagen [26,27]. The chondrocytes dedifferentiate and change their phenotypes. Three-dimensional microenvironments are necessary to promote cell differentiation [28,29]. Micromass pellet culture is often used in the basic study of the chondrogenic differentiation capacity of MSCs. The formation of pellets on PAAm-, PAAc-, PEG-modified, and control surfaces in the present study should provide additional information regarding the chondrogenic differentiation of MSCs.

5. Conclusions

The electrostatic properties of a biomaterial surface could affect cell functions such as cell adhesion,

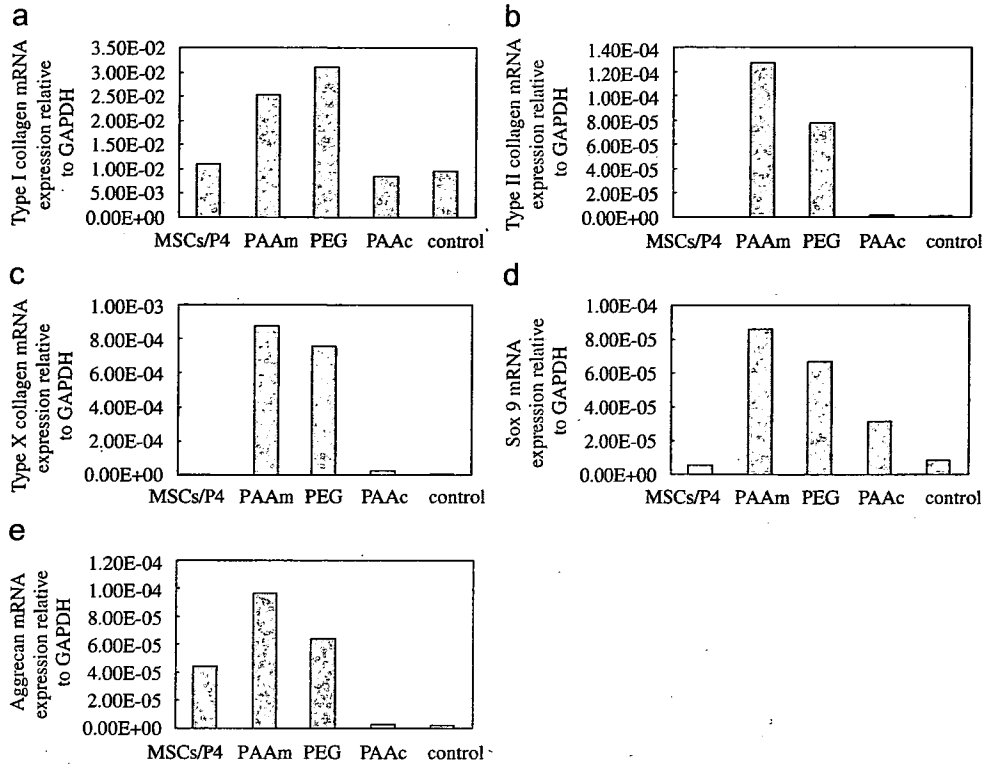

Fig. 7. Real-time PCR results of mRNA expression of type I collagen (a), type II collagen (b), type X collagen (c), sox 9 (d), and aggrecan (e) of the MSCs cultured on PAAm-, PEG-, PAAc-modified and control surfaces in chondrogenic induction medium for 2 weeks. The data are normalized to GAPDH. MSCs/P4 is the cells seeded onto the surfaces.

proliferation, and differentiation. The positively charged PAAm-modified surface supported cell adhesion, proliferation, and the chondrogenic differentiation of MSCs. The negatively charged and control surfaces supported cell adhesion and proliferation, but not chondrogenic differentiation. The neutral PEG-modified surface supported neither cell adhesion nor proliferation, but did promote chondrogenic differentiation. Although both the PAAm- and PEG-modified surfaces promoted chondrogenic differentiation of MSCs, the PAAm-modified surface supported cell adhesion whereas the PEG-modified surface did not. The positively charged PAAm-modified surface is more appealing for tissue engineering because, at first, it can support cell adhesion, and then switch to differentiation of the proliferated cells. Thus, cell proliferation and differentiation could occur on the same surface at different times. Consequently, cell differentiation could be controlled by changing the surface properties such as the electrostatic property. The results of this study will provide important information for the design of scaffolds for tissue engineering.

Acknowledgments

We are grateful to Mrs. Yumie Imaizumi for her assistance in real-time PCR analysis. This work was supported in part by the New Energy and Industrial Technology Development Organization of Japan and in part by the Ministry of Education, Culture, Sports, Science and Technology of Japan.

References

[1] Woodfield TB, Miot S, Martin I, van Blitterswijk CA, Riesle J. The regulation of expanded human nasal chondrocyte re-differentiation capacity by substrate composition and gas plasma surface modification. Biomaterials 2006;27(7):1043–53.
[2] Keselowsky BG, Collard DM, Garcia AJ. Integrin binding specificity regulates biomaterial surface chemistry effects on cell differentiation. Proc Natl Acad Sci USA 2005;102:5953–7.
[3] Flemming RG, Murphy CJ, Abrams GA, Goodman SL, Nealey PF. Effects of synthetic micro- and nano-structured surfaces on cell behavior. Biomaterials 1999;20(6):573–88.
[4] Singhvi R, Kumar A, Lopez GP, Stephanopoulos GN, Wang DI, Whitesides GM, et al. Engineering cell shape and function. Science 1994;264:696–8.
[5] Prime KL, Whitesides GM. Self-assembled organic monolayers: model systems for studying adsorption of proteins at surfaces. Science 1991;252:1164–7.
[6] Mahmood TA, Miot S, Frank O, Martin I, Riesle J, Langer R, et al. Modulation of chondrocyte phenotype for tissue engineering by designing the biologic–polymer carrier interface. Biomacromolecules 2006;7(11):3012–8.
[7] Mahmood TA, de Jong R, Riesle J, Langer R, van Blitterswijk CA. Adhesion-mediated signal transduction in human articular chondrocytes: the influence of biomaterial chemistry and tenascin-C. Exp Cell Res 2004;301:179–88.
[8] Papadaki M, Mahmood T, Gupta P, Claase MB, Grijpma DW, Riesle J, et al. The different behaviors of skeletal muscle cells and chondrocytes on PEGT/PBT block copolymers are related to the

surface properties of the substrate. J Biomed Mater Res 2001;54: 47–58.
[9] Keselowsky BG, Collard DM, Garcia AJ. Integrin binding specificity regulates biomaterial surface chemistry effects on cell differentiation. Proc Natl Acad Sci USA 2005;102(17):5953–7.
[10] Lan MA, Gersbach CA, Michael KE, Keselowsky BG, Garcia AJ. Myoblast proliferation and differentiation on fibronectin-coated self assembled monolayers presenting different surface chemistries. Biomaterials 2005;26(22):4523–31.
[11] Scotchford CA, Gilmore CP, Cooper E, Leggett GJ, Downes S. Protein adsorption and human osteoblast-like cell attachment and growth on alkylthiol on gold self-assembled monolayers. J Biomed Mater Res 2002;59:84–99.
[12] McClary KB, Ugarova T, Grainger DW. Modulating fibroblast adhesion, spreading, and proliferation using self-assembled monolayer films of alkylthiolates on gold. J Biomed Mater Res 2000;50: 428–39.
[13] Scotchford CA, Cooper E, Leggett GJ, Downes S. Growth of human osteoblast-like cells on alkanethiol on gold self-assembled monolayers: the effect of surface chemistry. J Biomed Mater Res 1998;41:431–42.
[14] Tidwell CD, Ertel SI, Ratner BD. Endothelial cell growth and protein adsorption on terminally functionalized, self-assembled monolayers of alkanethiolates on gold. Langmuir 1997;13:3404–13.
[15] Curran JM, Chen R, Hunt JA. The guidance of human mesenchymal stem cell differentiation in vitro by controlled modifications to the cell substrate. Biomaterials 2006;27(27):4783–93.
[16] Curran JM, Chen R, Hunt JA. Controlling the phenotype and function of mesenchymal stem cells in vitro by adhesion to silane-modified clean glass surfaces. Biomaterials 2005;26(34):7057–67.
[17] Sugawara T, Matsuda T. Synthesis of phenylazido-derivatized substances and photochemical surface modification to immobilize functional groups. J Biomed Mater Res 1996;32(2):157–64.
[18] Hasuda H, Kwon OH, Kang IK, Ito Y. Synthesis of photoreactive pullulan for surface modification. Biomaterials 2005;26(15):2401–6.
[19] Ito Y. Surface micropatterning to regulate cell functions. Biomaterials 1999;20(23–24):2333–42.
[20] Labarca C, Paigen K. A simple, rapid, and sensitive DNA assay procedure. Anal Biochem 1980;102:344–52.
[21] Brown AN, Kim BS, Alsberg E, Mooney DJ. Combining chondrocytes and smooth muscle cells to engineer hybrid soft tissue constructs. Tissue Eng 2000;6:297–305.
[22] Matin I, Jakob M, Schafer D, Spagnoli G, Heberer M. Quantitative analysis of gene expression in human expression in human articular cartilage from normal and osteoarthritic joints. Osteoarthr Cartil 2001;9:112–8.
[23] Schaefer JF, Millham ML, de Crombrugghe B, Buckbinder L. FGF signaling antagonizes cytokine-mediated repression of sox9 in SW1353 chrondrosarcoma cells. Ostioarthr Cartil 2003;11:233–41.
[24] Keselowsky BG, Collard DM, Garcia AJ. Surface chemistry modulates fibronectin conformation and directs integrin binding and specificity to control cell adhesion. J Biomed Mater Res 2003; 66A:247–59.
[25] Keselowsky BG, Collard DM, Garcia AJ. Surface chemistry modulates focal adhesion composition and signaling through changes in integrin binding. Biomaterials 2004;25(28):5947–54.
[26] Chen G, Sato T, Ushida T, Hirochika R, Tateishi T. Redifferentiation of dedifferentiated bovine chondrocytes when cultured in vitro in a PLGA–collagen hybrid mesh. FEBS Lett 2003;542:95–9.
[27] von der Mark K, Gauss V, von der Mark H, Muller P. Relationship between cell shape and type of collagen synthesised as chondrocytes lose their cartilage phenotype in culture. Nature 1977; 267:531–2.
[28] Johnstone B, Hering TM, Caplan AI, Goldberg VM, Yoo JU. In vitro chondrogenesis of bone marrow-derived mesenchymal progenitor cells. Exp Cell Res 1998;238:265–72.
[29] Benya PD, Shaffer JD. Dedifferentiated chondrocytes reexpress the differentiated collagen phenotype when cultured in agarose gels. Cell 1982;30:215–24.

Covalently immobilized biosignal molecule materials for tissue engineering

Yoshihiro Ito

Received 1st June 2007, Accepted 5th September 2007
First published as an Advance Article on the web 8th October 2007
DOI: 10.1039/b708359a

Immobilization of biosignal molecules including growth factors and cytokines is important for developing biologically active materials which can contribute to tissue engineering as a component. The immobilization has more meanings than only immobilization of the enzyme in a bioreactor or ligand–receptor interactions, because the immobilized biosignal molecules work on cells which have very complex structures and functions. This review discusses recent progress in immobilization of biosignal molecules, including the mechanisms and design concepts.

1. Introduction

Current clinical technologies, especially donor transplants and artificial organs, have been excellent life-saving and life-extending therapies to treat patients who need to reconstitute diseased or devastated organs or tissues as a result of an accident, trauma, and cancer, or congenital structural anomalies. Although advances in surgical techniques, immunosuppression, and postoperative care have improved survival and quality of life, there are still problems associated with the use of biological grafts, such as donor site morbidity, donor scarcity, and tissue rejection. A variety of synthetic and natural materials have been developed for the replacement of lost tissues, but the results have not been satisfactory. Tissue engineering has emerged as a promising alternative in which organs or tissue can be repaired, replaced, or regenerated.[1]

In tissue engineering, a neotissue is generally generated from the cells on a bioresorbable scaffold, incorporating growth factors as shown in Fig. 1. It can consist of up to three components: cells, scaffold, and growth factors. Recent progress in cell biology revealed various types of stem cell. However, because of the scarcity of stem cells it is important to increase the number of stem cells for clinical utilization. Bioreactors to amplify the stem cells are required and, for the construction of bioreactors, some novel materials which enhance the growth or differentiation are desired.[2–6]

For the design of biomaterials, cells and proteins at the interface play an important role.[7,8] Especially for the development of such bioreactor materials or bioactive materials to enhance regeneration in the body, the utilization of biosignal proteins including growth factors and cytokines is reasonable. However, although there are many examples of material design to enhance cell adhesion, there are not so many investigations for regulation of various higher functionalities (gene expression) of cells including growth, differentiation, apoptosis, transformation and so on. In this review the possibilities for regulating the expression of cells by materials are discussed.

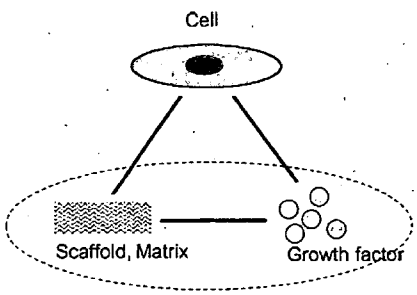

Fig. 1 The principle of tissue engineering. This review focuses on the fusion, that is, immobilization of growth factor on the scaffold.

Nano Medical Engineering Laboratory, RIKEN (The Institute of Physical and Chemical Research), 2-1 Hirosawa, Wako-shi, Saitama 351-0198, JAPAN

Yoshihiro Ito

Yoshihiro Ito received his Bachelor's (1981) and Master's (1983) degrees in Polymer Chemistry from Kyoto University and was awarded a Doctorate in Engineering from the same university in 1987. Since then he has held a number of posts at various institutions including Research Fellow of the Japan Society for the Promotion of Science (1987), Assistant (1988) and Associate (1996) Professor at Kyoto University, Research Fellow at the University of California, Irvine (1992–1993), Professor at the University of Tokushima (1999), and Project Leader at the Kanagawa Academy of Science and Technology (2002–2007). Now, he is Chief Scientist and Director of the Nano Medical Engineering Laboratory at the RIKEN Institute of Physical and Chemical Research (since 2004). His research focuses on biomaterials science, regenerative medical engineering, combinatorial bioengineering for the creation of functional polymers, and soft nanotechnology.

 This journal is © The Royal Society of Chemistry 2008

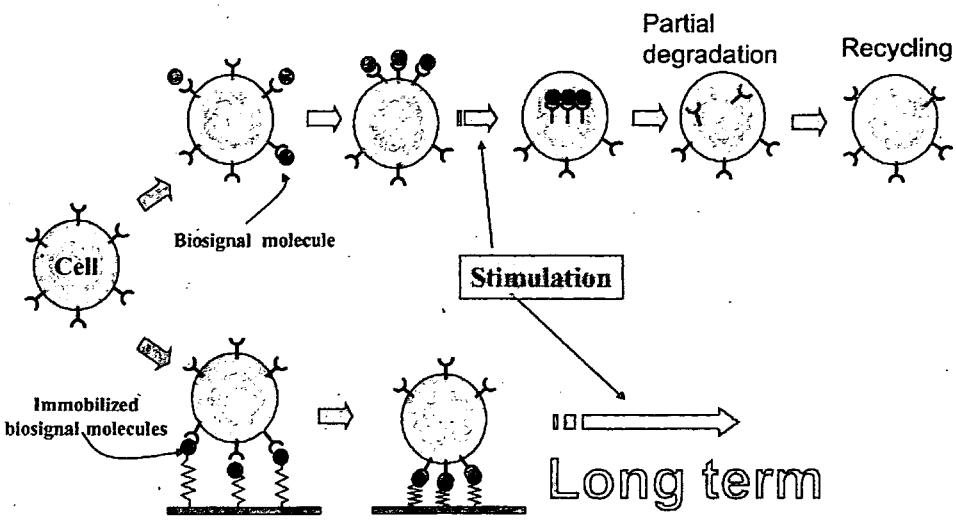

Fig. 2 Interaction of cells with soluble and immobilized growth factors.

2. Immobilization of biosignal molecules

Fig. 2 shows the activation mechanism of biosignal molecules including growth factors and cytokines. First, the biosignal molecules interact with the cognate receptor and form a complex with it, resulting in autophosphorylation of the cytoplasmic domains of the receptors. The phosphorylation activates the intracellular signal transduction. On the other hand, the formed complexes are aggregated and the aggregates are internalized into cells. The internalization occurs by both clathrin-dependent and clathrin-independent mechanisms and leads to the recycling of receptors to the plasma membrane for resensitization or shuttling of receptors to lysosomes for degradatory down-regulation.

If the signal transduction from biosignal molecules to cells is due to complex formation with the receptor, it is expected that the biosignal molecules immobilized on the material surface work. In addition, it is expected that the signal transduction by the immobilized molecules continues for a longer time than by the soluble molecules.

2.1. History of immobilized growth factor

Immobilization of insulin on a solid matrix was for the first time performed and reported by Cuatrecasas.[9] He synthesized the conjugates to investigate the mechanism of insulin action. Although these conjugates facilitated extensive purification of solubilized insulin receptors by affinity chromatography, definitive conclusions regarding the effectiveness of immobilized insulin could not be drawn because of the possibility that the immobilization was incomplete.[10–15] Furthermore, given the marked time delay between the exposure of the cells to the immobilized insulin and the detection of signal transduction events, his study examining acute effects of insulin conjugates may not have allowed sufficient time for evaluation of activity. In addition, because his studies used porous agarose gel beads that were not accessible to the cells as the immobilizing support, it was difficult to evaluate quantitatively the relationship between the amount of immobilized insulin and biological activities.

After these works, in 1991 insulin was immobilized on a plain surface as a growth factor for investigation of its mitogenic (a long-term) effect.[16,17] Subsequently various types of biosignal molecules have been immobilized on materials to regulate cell functions. Table 1 summarizes reports on bioconjugate materials which were covalently immobilized with growth factors to regulate cellular functions.[18–109] Immobilized insulin and epidermal growth factor (EGF) enhanced the growth of cells.[16–65] Bone morphogenetic protein (BMP) −2 or −4 induced alkaline phosphatase activity, or calcium deposition, or regulated gene expression in cells.[73–77] The immobilized transforming growth factor-β1 (TGF-β1) induced collagen synthesis[86,89] or suppressed chondrocytes toward prehypertrophic chrondrocytes and osteolineage cells.[88] Notch ligands induced Notch activation in cells only in the immobilized state and it was suggested to expand human hematopoietic stem cell population.[93–95] Immobilization of leukemia inhibitory factor (LIF) kept the colony morphology, alkaline phosphatase activity, and stage-specific embryonic antigen-1 immunoreactivity of embryonic stem cells, which indicated an undifferentiated state.[96,97]

On the other hand, in around 1990, in the field of cell biology, biologically natural "juxtacrine stimulation", which indicates biological signal transduction in a nondiffusible manner to neighboring cells, was demonstrated for some membrane-anchored growth factors and lymphokines, including TGF-α, tumor necrosis factor α, colony-stimulating factor 1, c-kit ligand, and heparin-binding EGF.[110,111] Considering the biological system, Ito *et al.* named the effect induced by a chemically immobilized growth factor "artificial juxtacrine stimulation".[112] Recently, some reviews for biomimetic approaches to biomaterials, which signal to cells *via* biologically active entities, have been published.[7,113]

2.3. Interaction of immobilized growth factor

In order to demonstrate that the immobilized signal molecules work to transduce the signal to the cells, some works have been performed. Chen *et al.*[27] prepared three basic types of insulin

Table 1 Biosignal molecules covalently immobilized on a matrix for cell culture

Growth factor	Substrate	Reference
Insulin	Surface-hydrolyzed poly(methyl methacrylate) (PMMA)	16–21
	Surface-treated glass or polyacrylamide	22
	Polyurethane	23
	Biodegradable polymer	24
	Poly(2-hydroxyethyl methacrylate) (poly(HEMA))	25
	Spacer, surface-treated PMMA with POE	26
	Polymer grafted with poly(acrylic acid)	27, 28
	Polyurethane with POE	29
	Biodegradable polymer + POE	30–32
	+ Adhesion factors (RGDS (Arg-Gly-Asp-Ser), pollyallylamine, collagen, *etc.*)	33–40
	+ Heparin	41
	Polystyrene + micropatterning	42, 43
	Poly(*N*-isopropylacrylamide)	44
	Poly(*N*-isopropylacrylamide) + RGDS	45–47
Epidermal growth factor (EGF)	Surface-modified glass	48–50
	Surface-hydrolyzed PMMA	51
	Surface-modifed PDMS	52, 53
	Polystyrene photo-immobilized (mircopatterned)	54–59
	Gene-engineered	60–66
Nerve growth factor (NGF)	Surface-modified glass	49, 67
	Poly(HEMA) grafted with PAA	68, 69
	Gelatin tricalcium phosphate crosslinked	70
	Micropatterned	71, 72
Bone morphogen protein (BMP)	Surface-modified titanium	73, 74
	Type I atelocollagen	75, 76
	Chitosan nanofiber	77
	Poly(lactide-*co*-glycolide)	78
Vasular endothelial growth factor (VEGF)	PAA-grafted polyethylene film	79
	Micropatterned	80
	Gene-engineered	81
Fibroblast growth factor (FGF)	Photoimmobilization	82
	Polymers	83
	+ Heparin	84, 85
Insulin growth factor-1 (IGF-1)	Photoimmobilization	82
Transforming growth factor-β1 (TGF-β1)	Collagen type I coated titanium	86
	PDMS	87
	Gelatin-hyaluronic acid-chondroitin-6-sulfate sponge	88
	+ POE	89
Hapatocyte growth factor (HGF)	Gene-engineered	90, 91
Notch ligand	Photo-immobilized	92
	Gene-engineered	93–95
Leukemia inhibitory factor (LIF)	Photo-immobilized	96
	Non-woven polyester fabrics	97
Stem cell growth factor (SCF)	Gene-engineered	98
Interleukin-2	Crosslinked	99
Interleukin-1	Gene-engineered	100
Tumor necrosis factor-α (TNF-α)	Photo-immoblized	67,101
Erythropoetin	Photo-immobilized with gelatin	102
Neurotrophin-3	Surface-modified glass	50
Transferrin	Surface-hydrolyzed PMMA	103
E-cadherin	Gene-engineered	104

This journal is © The Royal Society of Chemistry 2008

Table 1 Biosignal molecules covalently immobilized on a matrix for cell culture (*Continued*)

Growth factor	Substrate	Reference
Osteopontin	Poly(2-hydroxyethyl methacrylate)	105
	Collagen	106
P-selectin	Coated on polystyrene	107
CXCR3 ligand	Coated on polystyrene	108
Sonic hedgehog	Gene-engineered + interpenetrating polymer network	109

conjugate and their effect on cell growth was investigated. The insulin–polyoxyethylene conjugate (Ins–POE), insulin–poly(acrylic acid) conjugate (Ins–PAA), and insulin–immobilized PAA-grafted polystyrene (Ins–PSt). Ins–POE and Ins–PAA were monovalent and multivalent water-soluble conjugates, respectively. On the other hand, Ins–PSt was a water-insoluble multivalent conjugate. The mitogenic activity of Ins–POE was lower than that of native insulin. This could be due to the inability of the insulin receptor to bind to the coupled insulin because of steric hindrance from the polyoxyethylene chain. With similar reasoning, poly(acrylic acid) should inhibit the binding of insulin to its receptor. However, Ins–PAA showed a slightly higher mitogenic activity compared to native insulin, presumably because Ins–PAA was multivalent and hence able to enhance receptor dimerization as well as aggregation of the insulin conjugate/receptor complex. On the other hand, Ins–PSt had an extremely high mitogenic effect being much higher than the other conjugates. Similar results were obtained using different types of matrix[28] and using the immobilized EGF[51] as summarized in Fig. 3.

2.4. Certification of the interactions

As discussed previously,[10–15] in the case of immobilization of biosignal molecules on a solid, the completeness is very important. If there are some releases from the matrix, the effect may be due to some artifact. Therefore the amount of immobilized insulin was carefully measured by radioisotope labeling.[20] In addition, the immobilized growth factor was repeatedly used after each cell culture.[21–102] This repeated use confirms the stability of the immobilized molecules. In addition to these methods, there are some technologies to demonstrate the activity of immobilized biosignal molecules.[14]

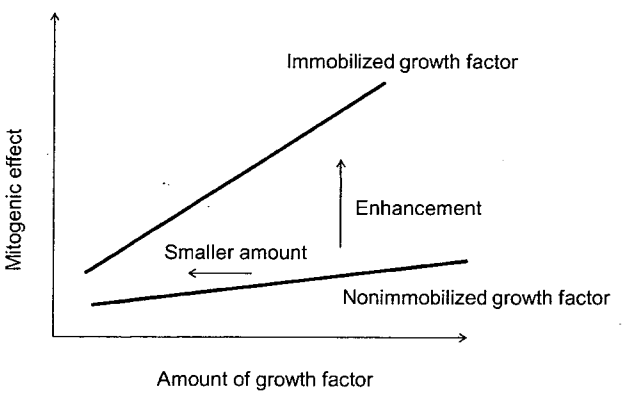

Fig. 3 Schematic comparison of the mitogenic effect of immobilized growth factor with that of nonimmobilized growth factor. Immobilized growth factor induces a greater effect than nonimmobilized growth factor. The smaller amount of immobilized growth factor is considered to induce the effect as a result of multivalency and high local concentration, as discussed in sections 3.1 and 3.3, respectively. The enhancement of the mitogenic effect is considered to be caused by inhibition of down-regulation and other factors as discussed in sections 3.2 and 3.3, respectively.

Specific interaction of immobilized growth factor with the cognate receptor was examined by antibodys against immobilized growth factor. If the effect of the immobilized growth factor was inhibited by the antibody, the specific interactions were certified. This method has been employed by many researchers.[14,19,80,110,111]

One of the technologies to certify the interactions, visualization of the signal transduction and spatial regulation of the cell functions, was performed by micropattern-immobilization using a photo-lithographic method.[42,43,54–59,67,71,72,80,92,102] When the cell culture was on the micropattern-immobilized growth factor, the cell growth or differentiation was accelerated only in the biosignal molecule-immobilized areas. The immobilized biosignal molecules affected the cell functions including growth and differentiations without enhancing the adhesion.

To further investigate the interaction of immobilized EGF, CHO cells overexpressing EGF receptors were cultured on the plate immobilized with EGF in a narrow stripe pattern.[55] The contact area (stripes 2 μm in width) between the cells and the immobilized EGF was stained by an anti-phosphotyrosine antibody. Since free lateral diffusion and internalization of the bound EGF–EGF receptor complex were prohibited by immobilization of EGF, only signal proteins in the interaction regions were activated. This finding also indicates that the biological signal was transduced only to the cell that interacted with the immobilized EGF.

Recently Ichinose *et al.*[49] quantitatively evaluated the interaction. When the density of EGF was only slightly lower than that of the EGF receptor dimers, cellular response was dramatically decreased. The EGF receptor molecules bound with the immobilized EGF were prevented from being laterally diffused and internalized and kept their initial position. In addition, the immobilization made suitable targets for stable single molecule observation under total internal reflection fluorescence microscopy to study EGF signaling mechanisms, preventing lateral diffusion and internalization of EGF receptors. Ichinose *et al.* showed results of single molecule observations of the association and dissociation between phosphorylated EGF receptors and Cy3-labeled growth factor

receptor-binding protein 2 (Grb2) proteins in A431 cells stimulated by the immobilized EGF.

Shibata *et al.*[67] demonstrated that nerve growth factor (NGF)–receptor complexes had two distinct diffusive states, characterized as a mobile and an immobile phase. The transition between the two diffusive states occurred reversibly with duration times determined by a single rate limiting process. The abrupt transition to the immobile phase often occurred simultaneously with the clustering of the NGF–receptor complexes. Immobilization depended on the phosphorylation of the TrkA NGF–receptor. Using dual-color imaging, it was demonstrated that the membrane recruitment of the intercellular signaling protein occurs with NGF–receptor complexes in the immobile phase indicating that signal transduction occurs during this phase. Thus, it was considered that NGF signaling was performed through a repetitive random process to induce formation of signaling complexes.

Previously the effect of immobilized growth factor was compared with the effect of adhesion factors including gelatin, collagen, and fibronection, or with albumin, immunoglobulin.[18] Recently microarray systems have been employed to investigate the effect of immobilized molecules by some researchers.[50,82,114,115] The recently developed systems also revealed the effectiveness of immobilized growth factors. At least the result that the immobilized biosignal molecules stimulate the cells has been confirmed by many methods.

3. Effect accompanying immobilization of growth factors

In addition to the fact that the immobilized growth factors interact with the cellular cognate receptors, it has been demonstrated that the immobilized growth factor had a higher or different effect from the soluble one as shown in Fig. 3, because the interaction is not only the ligand–receptor interaction. These effects of immobilized growth factor are considered to be due to the following mechanisms.[21]

3.1. Multivalency

The importance of mutivalency of immobilized biosignal molecules have been discussed by many researchers. This effect is the same as the high local concentration of immobilized proteins on material surfaces.[16,116] Recently Kiessling *et al.* considered synthetic multivalent ligands as probes of signal transduction.[117] Multivalent ligands can bind avidly to multiple receptors on the cell surface, a process that is facilitated in the fluid lipid bilayer by the two dimensional diffusion of receptors. The multivalent ligands can activate signaling pathways if they can cluster signaling receptors (Fig. 4). They discussed the three major concepts that are critical for the application of multivalent ligands as probes of signal transduction: (1) signal transduction cascades are mediated by receptor–receptor interactions, and promoting receptor assembly is critical for signaling. (2) Multivalent ligands can interact with the target receptors through multiple binding modes. (3) The structure of a multivalent ligand will determine the favored binding modes. Thus, the structure can be optimized to elicit the desired biological response.

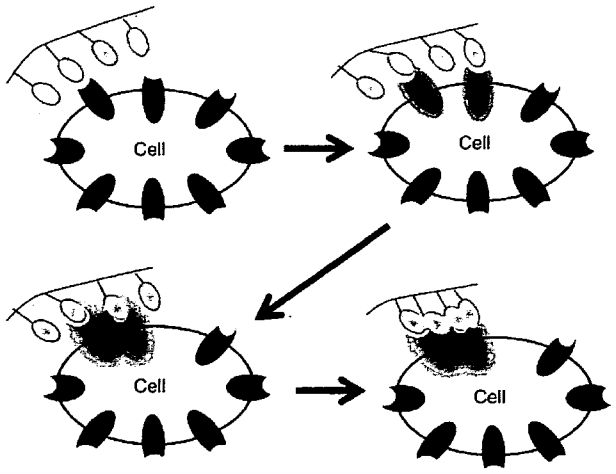

Fig. 4 Interactions of a multivalent ligand with a cell. The multivalent ligand enhances the formation of ligand–receptor complexes, and the interaction of activated ligand–receptor complexes, because of the high local concentration of ligands. In addition, the formed complexes are stabilized by the multivalent ligands.

In addition, prevention of lateral diffusion of the activated receptor or the receptor–ligand complex in the plane of the cell membrane must be taken into consideration. The prevention means the stabilization of the aggregates of complexes and thus leads to a long-lasting effect.

3.2. Inhibition of down-regulation

Inhibition of the internalization process should be also taken into consideration as shown in Fig. 2. Generally cells decompose the biosignal molecules in the cells to reduce their stimulation and this is called down-regulation. The immobilization was considered to inhibit this down-regulation and as a result the stimulation continued for a long time without reduction.

To investigate the above hypothesis, the activation of cellular signaling proteins, insulin receptor β-subunits in the cells, or mitogen-activated protein kinase (MAPK) in the cells was measured in the presence of immobilized insulin or immobilized EGF (Fig. 5).[21,51] Native insulin or EGF rapidly activated the insulin or EGF receptor. However, the activation is usually transient. On the other hand, activation by the immobilized insulin or EGF continued to increase up to 12 h although some lag time was needed for adhesion of cells on the surface immobilized with insulin or EGF. These sustained activations of signaling proteins by the immobilized insulin or EGF should explain the high mitogenic effect of the immobilized growth factors.

In addition, this sustained activation provided another effect of immobilized biosignal molecules.[58] It is well known that growth of the rat phaeochromaocytoma cell line PC12 is stimulated by EGF and the differentiation is stimulated by NGF.[118] However, the immobilized EGF stimulated PC12 differentiation.[58] The immobilized EGF caused a long-lasting stimulation of MAPK and a subfamily of the MAPK superfamily in cells, as did diffusible NGF. This switching between growth stimulation and differentiation was considered to be due to the duration of stimulus.[58]

This journal is © The Royal Society of Chemistry 2008

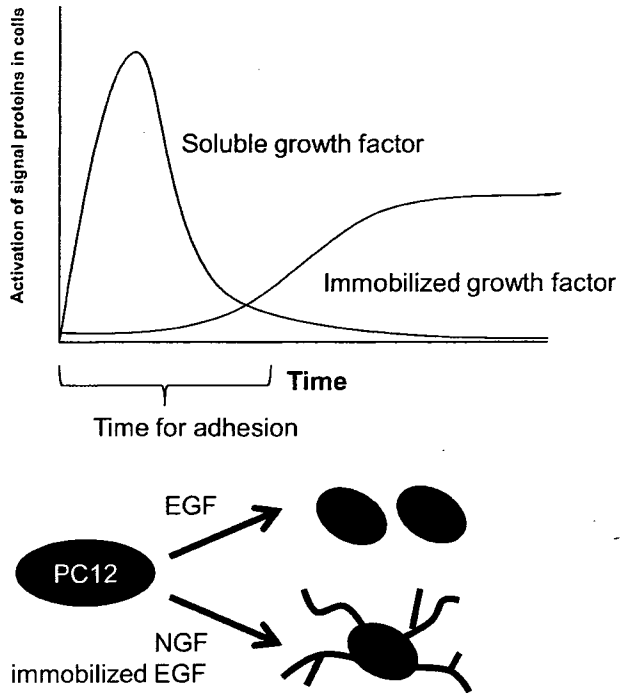

Fig. 5 Time course of signal activation by immobilized and soluble growth factors. The difference induces different effects on PC12 cells.

3.3. Other considerable mechanisms

In addition, the difference in stimulation sites between the cell–medium interface and cell–matrix interface, *etc.* should also be taken into consideration. The interaction of immobilized biosignal molecules is from the substrate and the local concentration is extremely high as shown in Fig. 6. The specific situation is considered to affect various functions.

In fact, the immobilization sometimes induced some specific effect on cell behavior in addition to the primary effect. Kuhl and Griffith-Cima[48] found that the rounding responses of primary rat hepatocytes on the surface immobilized with EGF were different to those on the non-immobilized. Ogiwara *et al.*[63] reported that the cytoskeleton of A431 cells adhering to immobilized EGF-Fc (Fc is a fragment of immunoglobulin) was filopodia whereas that of the cells adhering onto collagen in the presence of soluble EGF was lammellipodia. In addition, Ogiwara *et al.*[64] found that interaction between photo-immobilized EGF and the receptor in the cells was independent of Mg^{2+} although integrin-mediated cell adhesion to natural exracellular matrices is dependent on Mg^{2+}. Phosphorylation of EGF receptors in A431 cells was induced by immobilized EGF the same as soluble EGF. DNA uptake of hepatocytes decreased with immobilized EGF whereas it increased with soluble EGF. Liver-specific functions of hepatocytes were maintained for 3 d by immobilized EGF whereas they were not maintained by soluble EGF, indicating that immobilized EGF follows a different signal transduction pathway from soluble EGF. These differences with immobilized growth factors compared to the soluble ones should be due to the complex structure of interfaces surrounding the cultured cells.

Reddy *et al.*[119] demonstrated an approach derived from understanding how the attenuation mechanisms including growth factor depletion and receptor down-regulation arise from ligand/receptor trafficking processes. A recombinant EGF mutant with reduced receptor binding affinity is a more potent mitogenic stimulus for fibroblasts than natural EGF because of its altered trafficking properties. Optimization of ligand binding parameters requires systemic integration of processes from the initial binding event to the final cellular response. Their experimental data showed that consideration of cellular trafficking processes is essential for an optimization effort. The immobilized growth factor may have a similar effect.

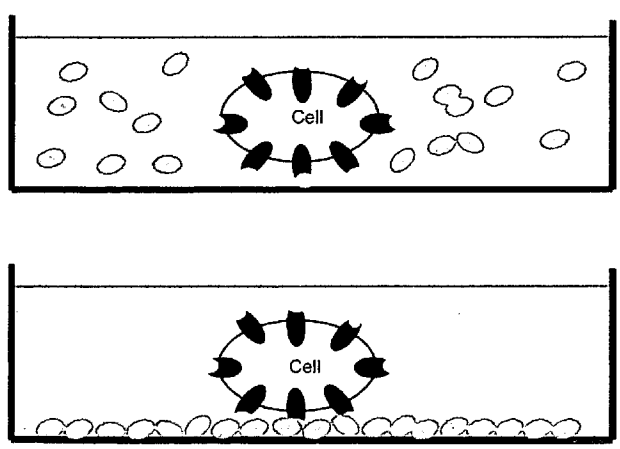

Fig. 6 Immobilized growth factor, which is different from soluble growth factor, provides a different environment for cells.

4. Design of immobilization

In order to efficiently derive the effect of immobilized biosignal molecules for material design, there are many strategies reported (Fig. 7).[120]

4.1. Spacer insertion and surface stiffness

As shown in Fig. 2, after the ligand complexes with the receptor, the complexes are generally considered to aggregate in the cell membrane to transmit the signal to the nuclei.

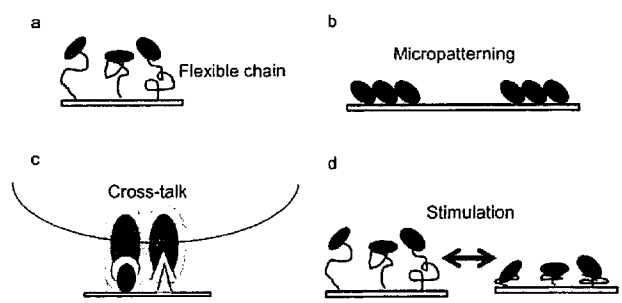

Fig. 7 Material designs using immobilized growth factors. (a) Flexible spacer chains make the immobilized growth factor mobile like a soluble growth factor. (b) Micropattern-immobilization for growth factors induces micropattern formation of cells. (c) Co-immobilization of different types of ligands (growth factor) induced cross-talk of receptors. (d) Stimuli-responsive polymers add some functions to the growth factor immobilization.

Therefore, the insertion of the spacer between the surface and the biosignal molecules is useful for enhancement of diffusion of the complex in the membrane. Some studies using the spacer chains were performed and the increase in the activity is reported.[26,29–32,48] However, possible implications of steric hindrance in spacing growth factor from the substrate and the possible impact on growth factor binding to its cell surface receptor should be taken into consideration. In fact, the POE conjugation reduced the biological activity of insulin.[27]

The insertion of a spacer arm is also related to the surface stiffness. It is well known that the cells sense and react to extracellular stiffness as revealed by recent experiments with soft elastic substrates.[121,122] Therefore, immobilization was performed on polymeric materials having different water contents and the effect of immobilized growth factor was discussed. The increase in flexibility of immobilized growth factor increased the biological activity.

Iwamoto and Mekada[111] discussed the juxtacrine mechanism according to the flexibility of membrane-anchored growth factor, heparin-binding epidermal growth factor (HB-EGF). Stable transfectants of mouse L cells expressing precursor HB-EGF (proHB-EGF) were fixed with formalin to prevent the release of soluble HB-EGF (sHB-EGF), and then the fixed donor cells were cultured with EP170.7 cells, an EGF receptor–ligand dependent cell line. Under these conditions, growth stimulation of EP170.7 cells was observed and this EP170.7 cell growth was found to be dependent on the amount of proHB-EGF expressed on the donor cells. On the other hand, in order to examine the activities of proHB-EGF, a modified coculture system was reported, in which an intact monkey kidney cell line expressing proHB-EGF was incubated with EGF receptor-expressing 32D cells. Under these conditions, proHB-EGF was shown to have a growth-inhibitory activity and to induce apoptosis of the recipient cells, while sHB-EGF stimulated cell growth. They consider that the fixation by formalin perturbed the aggregation of ligand/receptor complexes in the cell membrane.

4.2. Micropatterning

Biomaterials for cell patterning have been used to regulate cellular processes, such as proliferation and differentiation, through cellular adhesion.[120,123–132] As cells adhere to micropatterned substrates, they align themselves to the shape of the underlying adhesion region. This shape change induces changes in cytoskeleton features and has been shown to influence apoptosis and proliferation.[133] Gene expression and protein synthesis were also altered by changing the nuclear shape.[134] It has been determined that cell shape can also control stem cell differentiation[135] and that the tissue form itself can feed back to regulate patterns of proliferation through micromechanical forces.[136] Controlling the cellular microenvironment through micropatterning may be used for directing cell fate for tissue engineering applications.

Moreover, inside the body, cells lie in contact or in close proximity to other cell types in a tightly controlled architecture.[125] Tissue engineering constructs, which aim to reproduce the architecture and geometry of tissues, will benefit from methods of controlling cell–cell interactions within these tissues. Patterned cocultures are a useful tool for tissue engineering constructs and for studying cell–cell interactions *in vitro* because they can be used to control the degree of homotypic and heterotypic cell–cell contact. Pioneering work in this area was performed by studying the interaction of hepatocytes and nonparenchymal fibroblasts in cocultures.[137] Recently developed methods are based on thermally reversible polymers,[138] layer-by-layer deposition of ionic polymers,[139] microfluidic deposition,[140] and molding of hydrogels.[141]

As mentioned in section 3.1, the micropatterning is also useful for investigating the effect of immobilized growth factors. If no signal transduction is observed on non-immobilized growth factor, it is possible to conclude that there is no release of immobilized growth factor to act on the cells.[112,120]

In addition to the certification method, micropatterning has been employed for regulation of cellular morphology and tissue formation. Ito *et al.*[80] demonstrate the micropatterning of blood endothelial cells to form vessels. Gomez *et al.*[72] reported axon extension in neurons on the surface covalently immobilized with NGF and microtopography was introduced in the form of microchannels. When the two surface stimuli were presented in combination, a synergistic increase in axon length was detected, which could be a result of faster polarization triggered by topography plus enhanced growth from NGF.

4.3. Co-immobilization

In order to enhance the effect of immobilized growth factors, other macromolecules have been co-immobilized with them. Biological or physico-chemical enhancement of cell adhesion increased the mitogenic effect of immobilized growth factors.[33–40,45,46] For biological enhancement of cell adhesion, cell adhesion factors including collagen, fibronectin, gelatin, and the core RGDS peptide were co-immobilized. On the co-immobilized surface both adhesion and growth of cells were remarkably enhanced. For physico-chemical enhancement of cell adhesion, cationic polymers such as poly(allyl amine) and polylysine were employed.

In addition, recently various types of stimuli-responsive materials were developed and cells were manipulated on these materials.[142–145] Chen *et al.*[44] immobilized insulin with a thermo-responsive polymer, poly(*N*-isopropylacryamide). They observed growth enhancement by immobilized insulin and harvested the cells by lowering the temperature. Coimmobilization with insulin and RGDS peptide was reported by Hatakeyama *et al.*[45–47] recently.

4.4. Protein engineering for immobilization

Recently many types of gene-engineered proteins for immobilization have been reported. Nishi *et al.*[60] constructed fusion proteins consisting of a growth factor moiety and the collagen-binding domain (CBD) of collagenase, which acted as an anchor to the collagen fibrils. They chose EGF and basic fibroblast growth factor (bFGF) as parts of the fusion proteins (collagen-binding EGF, CBEGF; collagen-binding bFGF, CB-FGF). As a result, CBEGF, when injected subcutaneously into nude mice, remained at the sites of injection for up to 10 d, whereas EGF was not detectable 24 h after injection. Although

This journal is © The Royal Society of Chemistry 2008

CBEGF did not exert a growth-promoting effect *in vivo*, CBFGF, but not bFGF, strongly stimulated the DNA synthesis in stromal cells at 5 d and 7 d after injection. These results indicate that CBD may be used as an anchoring unit to produce fusion proteins nondiffusible and long-lasting *in vivo*.

Hayashi *et al.*[61] developed a recombinant technology to confer mitogenic activity on type III collagen by fusing it to EGF at the collagen's N-terminus. The fusion protein was shown to hold the triple helical conformation of collagen and the mitogenic activity of EGF. It was also demonstrated that the chimeric protein can be immobilized on tissue culture dishes as a fibrous form and in collagen fibrils without abolishing the original mitogenic activity of EGF.

Collagen-binding or fibrin-binding growth factors consisting of EGF, HGF, and VEGF and the binding domains in fibronectin were reported as shown in Fig. 8.[62,90] The fusion protein bound to gelatin and fibrillar collagen sponges and substantially stimulated cell growth after binding to collagen-coated culture plates, whereas EGF or HGF had no effect, indicating that this fusion protein acted as a collagen-associated growth factor. On the other hand, Elloumi *et al.*[65] reported a novel protein consisting of a RGD (Arg-Gly-Asp) sequence functioning as a cell adhesive function, EGF as a cell growth function, and a hydrophobic sequence as an efficient assembling function in one molecule. The protein coated on an unmodified hydrophobic surface of a cell culture plate (through the hydrophobic moiety) retained both cell adhesive activity (through the RGD sequence) and cell growth activity (through the EGF moiety).

Recently Kim *et al.*[100] prepared a fusion protein of a recombinant human interleukin-1 (IL-1) receptor antagonist and an elastin-like peptide (IL-1ra-ELP) and found that the immobilized IL-1ra-ELP modulates the inflammatory profile of lipopolysaccharide (LPS)-stimulated cultured human monocytes. Specifically LPS-stimulated THP-1 monocytes that were exposed to either soluble or immobilized IL-1ra-ELP did not differentiate, but showed attenuated expression of pro-inflammatory cytokines, and had enhanced production of anti-inflammatory and pro wound-healing cytokines. The extent of signaling by immobilized and soluble fusion proteins were similar in magnitude, indicating roughly equivalent bioactivity and that cultured monocytes are clearly signaled by the immobilized IL-1ra-ELP.

As another binding method, fusion with immunoglobulin G Fc region,[63] *p*-azido phenylalanine,[64] histidine tag,[66] cysteine-containing tag[81] and cellulose-binding domain[98] were employed. These gene engineering methods contributed oriented immobilization of biosignal molecules for efficient interaction with receptors to induce cellular signal transduction.

5. *In vivo* applications

Covalent immobilization of growth factor onto a substrate has been used mainly for cell culture. However, some *in vivo* experiments have also been performed for tissue engineering. Ohyama *et al.*[85] prepared bFGF-immobilized platinum microcoils and performed coil embolization of aneurysms constructed using a canine common carotid artery *via* the endovascular approach. The percentage of occlusion at the aneurysm orifice in animals treated with bFGF-immobilized coils was significantly greater than with unmodified coils. Liu *et al.*[78] immobilized BMP-2 on a poly(lactide-co-glycolide) scaffold and created bilateral, full-thickness cranial defects in rabbits to investigate the osteogenic effect of cultured mesenchymal stromal cells on bone regeneration *in vivo*. Histomorphometry and histology demonstrated that the BMP-2 conjugate enhanced bone formation after surgery. Nishi *et al.*[60] prepared collagen-binding EGF and injected it subcutaneously into nude mice. It remained at the sites of injection for up to 10 d, whereas EGF was not detectable 24 h after injection. In addition, collagen-binding FGF strongly stimulated the DNA synthesis in stromal cells at five and seven days after injection. Kitajima *et al.*[90] prepared collagen-binding HGF and its angiogenic activity in rat tissues was examined by subcutaneously implanting collagen sponges containing the binding HGF. Blood vessel formation in the sponges after seven days was four to six times more extensive when compared with the control sponges without any sample. Implanted sponges with native HGF did not show significant any difference from the controls. Recently, Ohkawara *et al.*[91] studied the re-endothelialization and neointimal formation in balloon-injured rat carotid arteries in the presence of HGF and binding HGF. The left common carotid artery of male Sprague Dawley rats was injured with an inflated balloon catheter, and treated with binding HGF, native HGF, or saline (control) for 15 min. Rats were injected with Evans blue and

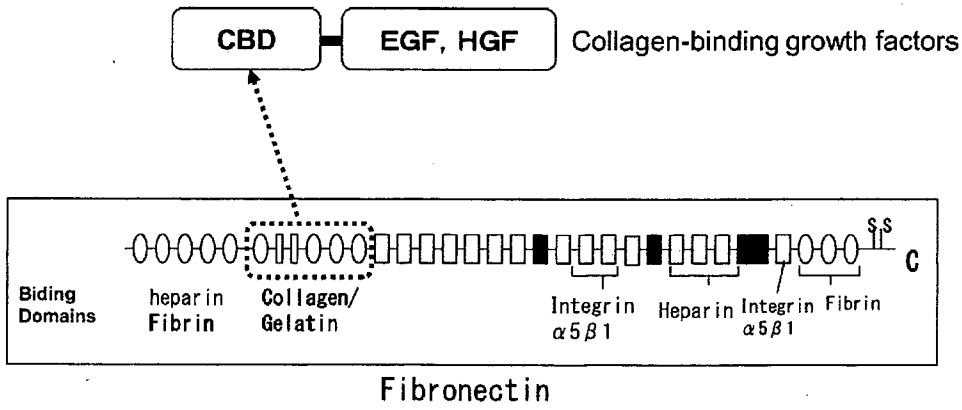

Fig. 8 Gene-engineered growth factors (EGF, VEGF, HGF, *etc.*) containing collagen-binding domain (CBD) found in fibronectin.

sacrificed after 14 d. The length of the re-endothelialized area was significantly longer in binding HGF-treated rats than in control or HGF-treated rats. Neointimal formation was significantly greater in binding HGF-treated rats than in others.

In tissue engineering, design of scaffold has been the main target. Growth factors are usually physically mixed for utilization. However, to effectively utilize the growth factors, modification is favored. Covalent or noncovalent immobilization regulates the diffusion of growth factors to maintain the effects and provide specific microenvironments to regulate cellular responses with matrices.[146–150] In addition, the immobilization of growth factor is important for geometrical control of complex tissue formation of different types of cells within or near the scaffolds.

6. Future perspective

The field of tissue engineering has created a need for biomaterials that are capable of providing biofunctional and structural support for living cells outside the body. Most of the commonly used biomaterials in tissue engineering are designed based on their physico-chemical properties, thus achieving precise control over mechanical strength, compliance, porosity, and degradation kinetics. Biofunctional signals are added to the scaffold by tethering, immobilizing, or supplementing biofunctional macromolecules, such as growth factors, directly to the scaffold material. The challenge in tissue engineering remains to find the correct balance between the biofunctional and the physical properties of the scaffold materials for each application.[151] Communication between cells and extracellular environment using the engineered scaffold should be correctly regulated. For this purpose the surface biolization by immobilization of growth factor is a powerful tool for constructing elaborate intelligent biofuntional materials. Control of surface function with the immobilization is important for design. It will be also important to prepare biomaterials mimicking the growth factor proteins for mass production of biofunctional materials without using the native proteins.

References

1 Y. Ikada, *Tissue Engineering: Fundamentals and Applications*, Elsevier, Oxford, UK, 2006.
2 G. J. M. Cabrita, B. S. Ferreira, C. L. da Silva, R. Concalves, G. Almeida-Porada and J. M. S. Cabral, *Trends Biotechnol.*, 2003, **21**, 233–240.
3 N. Panoskaltsis, A. Mantalaris and J. H. D. Wu, *J. Biosci. Bioeng.*, 2005, **100**, 28–35.
4 D. Marolt, A. Augst, L. E. Freed, C. Vepari, R. Fajardo, N. Patel, M. Gray, M. Farley, D. Kaplan and G. Vunjak-Novakovic, *Biomaterials*, 2006, **27**, 6138–6149.
5 Y. Ito, H. Hasuda, T. Kitajima and T. Kiyono, *J. Biosci. Bioeng.*, 2006, **102**, 467–469.
6 Y. Ito, M. Kawamorita, T. Yamabe, T. Kiyono and K. Miyamoto, *J. Biosci. Bioeng.*, 2007, **103**, 113–121.
7 Y. Hirano and D. J. Mooney, *Adv. Mater.*, 2004, **16**, 17–25.
8 J. Spatz, *Soft Matter*, 2007, **3**, 261–262.
9 P. Cuatrecasas, *Proc. Natl. Acad. Sci. U. S. A.*, 1969, **63**, 450–457.
10 R. W. Butcher, O. B. Croffird, S. Gammeltoff, J. Gilemann, J. R. Gavin, J. D. Goldfine, C. R. Kahn, M. Rodbell, J. Roth, L. Jarett, R. J. Lefkowitz, R. Levine and G. V. Marinetti, *Science*, 1973, **182**, 396–397.
11 T. Oka and Y. Topper, *Proc. Natl. Acad. Sci. U. S. A.*, 1974, **71**, 1630–1633.
12 H. J. Kolb, R. Renner, K. D. Weiss and O. H. Wieland, *Proc. Natl. Acad. Sci. U. S. A.*, 1975, **72**, 248–252.
13 P. Cuatrecasas, *Science*, 1973, **182**, 397–398.
14 J. C. Venter, *Pharmacol. Rev.*, 1982, **34**, 153–257.
15 J. L. Garwin and T. D. Gelehter, *Arch. Biochem. Biophys.*, 1974, **164**, 52–59.
16 Y. Ito, S. Q. Liu and Y. Imanishi, *Biomaterials*, 1991, **12**, 449–453.
17 S. Q. Liu, Y. Ito and Y. Imanishi, *Biomaterials*, 1992, **13**, 50–58.
18 Y. Ito, S. Q. Liu, M. Nakabayashi and Y. Imanishi, *Biomaterials*, 1992, **13**, 789–794.
19 S. Q. Liu, Y. Ito and Y. Imanishi, *J. Biochem. Biophys. Methods*, 1992, **25**, 139–148.
20 S. Q. Liu, Y. Ito and Y. Imanishi, *Enzyme Microb. Technol.*, 1993, **15**, 167–172.
21 Y. Ito, J. Zheng, Y. Imanishi, K. Yonezawa and M. Kasuga, *Proc. Natl. Acad. Sci. U. S. A.*, 1996, **93**, 3598–3601.
22 Y. Ito, T. Uno, S. Q. Liu and Y. Imanishi, *Biotechnol. Bioeng.*, 1992, **40**, 1271–1276.
23 S. Q. Liu, Y. Ito and Y. Imanishi, *J. Biomed. Mater. Res.*, 1993, **27**, 909–915.
24 Y. Ito, S. Q. Liu, T. Orihara and Y. Imanishi, *J. Bioact. Compat. Polym.*, 1994, **9**, 170–183.
25 I. K. Kang, S.-H. Choi, D.-S. Shin and S. C. Yoon, *Int. J. Biol. Macromol.*, 2001, **28**, 205–212.
26 Y. Ito, M. Inoue, S. Q. Liu and Y. Imanishi, *J. Biomed. Mater. Res.*, 1993, **27**, 901–907.
27 G. Chen, Y. Ito and Y. Imanishi, *Bioconjugate Chem.*, 1997, **8**, 106–110.
28 L. Bromberg and L. Salvati, Jr., *Bioconjugate Chem.*, 1999, **10**, 678–686.
29 E. J. Kim, I. K. Kang, M. K. Jang and Y. B. Park, *Biomaterials*, 1998, **19**, 239–249.
30 J. Tessmar, A. Mikos and A. Gopferich, *Biomaterials*, 2003, **24**, 4475–4486.
31 K. Kellner, J. Tessmar, S. Milz, P. Angele, M. Nerlich, M. B. Schulz, T. Blunk and A. Gopferich, *Tissue Eng.*, 2004, **10**, 429–440.
32 J. Tessmar, K. Kellner, M. B. Schulz, T. Blunk and A. Gopferich, *Tissue Eng.*, 2004, **10**, 441–453.
33 J. Zheng, Y. Ito and Y. Imanishi, *Biomaterials*, 1994, **15**, 963–968.
34 Y. Ito, J. Zheng and Y. Imanishi, *Biotechnol. Bioeng.*, 1995, **45**, 144–148.
35 J. Zheng, Y. Ito and Y. Imanishi, *J. Biomater. Sci., Polym. Ed.*, 1995, **7**, 515–522.
36 J. Zheng, Y. Ito and Y. Imanishi, *Biotechnol. Prog.*, 1995, **11**, 677–681.
37 J.-S. Li, Y. Ito, J. Zheng, T. Takahashi and Y. Imanishi, *J. Biomed. Mater. Res.*, 1997, **31**, 190–197.
38 Y. Ito, J. Zheng and Y. Imanishi, *Biomaterials*, 1997, **18**, 197–202.
39 M. Gumusdrelioglu and H. Turkoglu, *Biomaterials*, 2002, **23**, 3927–3935.
40 M. Gumusdrelioglu and A. G. Karakecili, *J. Biomater. Sci., Polym. Ed.*, 2003, **14**, 199–211.
41 Y. J. Kim, I. K. Kang, M. W. Huh and S. C. Yoon, *Biomaterials*, 2000, **21**, 121–130.
42 Y. Ito, G. Chen and Y. Imanishi, *Biotechnol. Prog.*, 1996, **12**, 700–703.
43 Y. Ito, S. Kondo, G. Chen and Y. Imanishi, *FEBS Lett.*, 1997, **403**, 159–162.
44 G. Chen, Y. Ito and Y. Imanishi, *Biotechnol. Bioeng.*, 1997, **53**, 339–344.
45 H. Hatakeyama, A. Kikuchi, M. Yamato and T. Okano, *Biomaterials*, 2006, **27**, 5069–5078.
46 H. Hatakeyama, A. Kikuchi, M. Yamato and T. Okano, *Inflammation Regener.*, 2006, **26**, 437–445.
47 H. Hatakeyama, A. Kikuchi, M. Yamato and T. Okano, *Biomaterials*, 2007, **28**, 3632–3643.
48 P. R. Kuhl and L. G. Griffith-Cima, *Nat. Med.*, 1996, **2**, 1022–1027.
49 J. Ichinose, M. Morimatsu, T. Yanagida and Y. Sako, *Biomaterials*, 2006, **27**, 3343–3350.

This journal is © The Royal Society of Chemistry 2008

50 M. Nakajima, T. Ishimuro, K. Kato, I.-K. Ko, I. Hirata, Y. Arima and H. Iwata, *Biomaterials*, 2007, **28**, 1048–1060.
51 Y. Ito, J.-S. Li, T. Takahashi, Y. Imanishi, Y. Okabayashi, Y. Kido and M. Kasuga, *J. Biochem.*, 1997, **121**, 514–520.
52 B. J. Klenkler, M. Griffith, C. Becerril, J. A. West-Mays and H. Sheardown, *Biomaterials*, 2005, **26**, 7286–7296.
53 B. J. Klenkler and H. Sheardown, *Biotechnol. Bioeng.*, 2006, **95**, 1158–1166.
54 G. Chen, Y. Ito and Y. Imanishi, *Biochim. Biophys. Acta*, 1997, **1358**, 200–208.
55 Y. Ito, G. Chen and Y. Imanishi, *Bioconjugate Chem.*, 1998, **9**, 277–282.
56 G. Chen, Y. Ito, S. Masuda and R. Sasaki, *Cytotechnology*, 2001, **35**, 3–8.
57 G. Chen and Y. Ito, *Biomaterials*, 2001, **22**, 2453–2457.
58 Y. Ito, G. Chen, Y. Imanishi, T. Morooka, E. Nishida, Y. Okabayashi and M. Kasuga, *J. Biochem.*, 2001, **129**, 733–737.
59 Y. K. Woo, S. Y. Kwon, H. S. Lee and Y. S. Park, *J. Orthop. Res.*, 2007, **25**, 73–80.
60 N. Nishi, O. Matsushita, K. Yuube, H. Miyanaka, A. Okabe and F. Wada, *Proc. Natl. Acad. Sci. U. S. A.*, 1998, **95**, 7018–7023.
61 M. Hayashi, M. Tomita and K. Yoshizato, *Biochim. Biophys. Acta*, 2001, **1528**, 187–195.
62 T. Ishikawa, H. Terai and T. Kitajima, *J. Biochem.*, 2001, **129**, 627–633.
63 K. Ogiwara, M. Nagaoka, C.-S. Cho and T. Akaike, *Biotechnol. Lett.*, 2005, **27**, 1633–1637.
64 K. Ogiwara, M. Nagaoka, C.-S. Cho and T. Akaike, *Biochem. Biophys. Res. Commun.*, 2006, **345**, 255–259.
65 I. Elloumi, R. Kobayashi, H. Funabashi, M. Mie and E. Kobatake, *Biomaterials*, 2006, **27**, 3451–3458.
66 T. Nakaji-Hirabayashi, K. Kato, Y. Arima and H. Iwata, *Biomaterials*, 2007, **28**, 357–3529.
67 S. C. Shibata, K. Hibino, T. Mashimo, T. Yanagida and Y. Sako, *Biochem. Biophys. Res. Commun.*, 2006, **342**, 316–322.
68 T. A. Kapur and M. S. Schoichet, *J. Biomater. Sci., Polym. Ed.*, 2003, **14**, 383–394.
69 T. A. Kapur and M. S. Schoichet, *J. Biomed. Mater. Res.*, 2004, **68A**, 235–243.
70 P. R. Chen, M. H. Chen, F. H. Lin and W. Y. Su, *Biomaterials*, 2005, **26**, 6579–6587.
71 Y. Ito, *Jpn. J. Artif. Organs*, 1998, **27**, 383–394.
72 N. Gomez, Y. Lu, S. Chen and C. E. Schmidt, *Biomaterials*, 2007, **28**, 271–284.
73 D. A. Puleo, R. A. Kissling and M. S. Sheu, *Biomaterials*, 2002, **23**, 2079–2087.
74 H. Schliphake, A. Aref, D. Scharnweber, S. Bierbaum, S. Roessler and A. Sewing, *Clin. Oral Impl. Res.*, 2005, **16**, 563–569.
75 H. Tsujigiwa, H. Nagatsuka, M. Gunduz, A. Rodriguez, A. J. Rivera, R. Z. Legeros, M. Inoue and N. Nagai, *J. Biomed. Mater. Res.*, 2005, **75**, 210–215.
76 H. Tsujigiwa, H. Nagatsuka, Y. J. Lee, P. P. Han, M. Gunduz, R. Z. LeGeros, M. Inoue, M. Yamada and N. Nagai, *J. Biomed. Mater. Res.*, 2006, **77A**, 507–511.
77 Y. J. Park, K. H. Kim, J. Y. Lee, Y. Ku, S. J. Lee, B. M. Min and C. P. Chung, *Biotechnol. Appl. Biochem.*, 2006, **43**, 17–24.
78 H.-W. Liu, C.-H. Chen, C.-L. Tsai, I-H. Lin and G.-H. Hsiue, *Tissue Eng.*, 2007, **13**, 1113–1124.
79 T. Taguchi, A. Kishida and M. Akashi, *J. Bioact. Compat. Polym.*, 2000, **15**, 309–320.
80 Y. Ito, H. Hasuda, H. Terada and T. Kitajima, *J. Biomed. Mater. Res.*, 2005, **74**, 659–665.
81 M. V. Backer, V. Patel, B. T. Jehning, K. P. Claffey and J. M. Backer, *Biomaterials*, 2006, **27**, 5452–5458.
82 K. Watanabe, T. Miyazaki and R. Matsuda, *Zool. Sci.*, 2003, **20**, 429–434.
83 S. Inoue and Y. Tabata, *Inflammation Regener.*, 2006, **26**, 181–184.
84 Y. Ito, M. Hayashi and Y. Imanishi, *J. Biomater. Sci., Polym. Ed.*, 2001, **12**, 367–378.
85 T. Ohyama, T. Nishide, H. Iwata, H. Sato, M. Toda, N. Toma and W. Taki, *J. Neurosurg.*, 2005, **102**, 109–115.
86 U. Fischer, U. Hempel, D. Becker, S. Bierbaum, D. Scharnweber, H. Worch and K. W. Wenzel, *Biomaterials*, 2003, **24**, 2631–2641.
87 K. Merret, C. M. Griffith, Y. Deslandes, G. Pleizier, M. A. Dube and H. Sherwood, *J. Biomed. Mater. Res.*, 2003, **67A**, 981–993.
88 C.-H. Chou, W. T. K. Cheng, C.-C. Lin, C.-H. Chang, C.-C. Tsai and F.-H. Lin, *J. Biomed. Mater. Res.*, 2006, **77B**, 338–348.
89 B. K. Mann, R. H. Schmedlen and J. L. West, *Biomaterials*, 2001, **22**, 439–444.
90 T. Kitajima, H. Terai and Y. Ito, *Biomaterials*, 2007, **28**, 1989–1997.
91 N. Ohkawara, H. Ueda, S. Shinozaki, T. Kitajima, Y. Ito, H. Asaoka, A. Kawakami, E. Kaneko and K. Shimokado, *J. Atheroscler. Thromb.*, 2007, **14**, 185–191.
92 T. Konno, S. Sakano, S. Higashida and Y. Ito, *Inflammation Regener.*, 2005, **25**, 426–430.
93 B. Varnum-Finney, L. Wu, M. Yu, C. Brashem-Stain, S. Staats, D. Flowers, J. D. Griffin and I. D. Bernstain, *J. Cell Sci.*, 2000, **113**, 4313–4318.
94 L. Vas V. Szilagyi, K. Paloczi and F. Uher, *J. Leukocyte Biol.*, 2004, **75**, 714–720.
95 B. L. Beckstead, D. M. Santosa and C. M. Giachelli, *J. Biomed. Mater. Res.*, 2006, **79A**, 94–103.
96 H. Makino, H. Hasuda and Y. Ito, *J. Biosci. Bioeng.*, 2004, **98**, 374–379.
97 G. Cetinkaya, H. Torkoglu, S. Arat, H. Odaman, M. A. Onur, M. Gumusderelioglu and A. Tumer, *J. Biomed. Mater. Res.*, 2007, **81A**, 911–919.
98 J. G. Doheny, E. J. Jervis, M. M. Guarna, R. K. Humphries, R. A. J. Warren and D. G. Kilburn, *Biochem. J.*, 1999, **339**, 429–434.
99 J. I. Horwitz, M. Toner, R. G. Tompkins and M. J. Yarmush, *Mol. Immunol.*, 1993, **30**, 1041–1048.
100 D. H. Kim, J. T. Smith, A. Chilkoti and W. M. Reichert, *Biomaterials*, 2007, **28**, 3369–3377.
101 Y. Guan, H. Zhong, X. Wang and T. Zhou, *Shengwu Yixue Gongchengxue Zazhi*, 2006, **23**, 346–349.
102 Y. Ito, H. Hasuda, T. Yamauchi, N. Komatsu and K. Ikebuchi, *Biomaterials*, 2004, **25**, 2293–2298.
103 S. Q. Liu, Y. Ito and Y. Imanishi, *Int. J. Biol. Macromol.*, 1993, **15**, 221–226.
104 M. Nagaoka, U. Koshimizu, S. Yuasa, F. Hattori, H. Chen, T. Tanaka, M. Okabe, K. Fukuda and T. Akaike, *PLoS ONE*, 2006, **e15**, 1–7.
105 S. M. Martin, R. Ganapathy, T. K. Kim, D. Leach-Scampavia, C. M. Giachelli and B. D. Ratner, *J. Biomed. Mater. Res.*, 2003, **67A**, 334–343.
106 S. M. Martin, J. L. Schwartz, C. M. Giachelli and B. D. Ratner, *J. Biomed. Mater. Res.*, 2004, **70A**, 10–19.
107 J. Koike, K. Nagata, S. Kudo, T. Tsuji and T. Irimura, *FEBS Lett.*, 2000, **477**, 84–88.
108 N. Kohrgruber, M. Groger, P. Meraner, E. Kriehuber, P. Petzelbauer, S. Brandt, G. Stingl, A. Rot and D. Maurer, *J. Immunol.*, 2004, **173**, 6592–6602.
109 J. E. Ho, E. H. Chung, S. Wall, D. V. Shaffer and K. E. Healy, *J. Biomed. Mater. Res.*, 2007, DOI: 10.1002/jbm.a.31355.
110 J. Massague and A. Pandiella, *Annu. Rev. Biochem.*, 1993, **62**, 515–541.
111 R. Iwamoto and E. Mekada, *Cytokine Growth Factor Rev.*, 2000, **11**, 335–344.
112 Y. Ito, G. Chen and Y. Imanishi, *J. Biomater. Sci., Polym. Ed.*, 1998, **9**, 879–890.
113 S. Drotleft, U. Lungwitz, M. Breunig, A. Dennis, T. Blunk, J. Tessmar and A. Gopferich, *Eur. J. Pharm. Biopharm.*, 2004, **58**, 385–407.
114 Y. Ito and M. Nogawa, *Biomaterials*, 2003, **24**, 3021–3026.
115 Y. Ito, *Biotechnol. Prog.*, 2006, **22**, 924–932.
116 R. Weissleder, K. Kelly, E. Y. Sun, T. Shtatland and L. Josephson, *Nat. Biotchnol.*, 2005, **23**, 1418–1423.
117 L. L. Kiessling, J. E. Gestwicki and L. E. Strong, *Angew. Chem., Int. Ed.*, 2006, **45**, 2348–2368.
118 S. Sasagawa, Y. Ozaki, K. Fujita and S. Kuroda, *Nat. Cell Biol.*, 2005, **7**, 365–373.
119 C. C. Reddy, S. K. Niyogi, A. Wells, H. S. Wiley and D. A. Lauffenburger, *Nat. Biotechnol.*, 1996, **14**, 1696–1699.
120 Y. Ito, *Biomaterials*, 1999, **20**, 2333–2342.
121 U. Schwarz, *Soft Matter*, 2007, **3**, 263–266.

122 I. Levental, P. C. Georges and P. A. Janmey, *Soft Matter*, 2007, **3**, 299–306.
123 P. P. Girard, E. A. Cavalcanti-Adam, R. Kemkemer and J. P. Spatz, *Soft Matter*, 2007, **3**, 307–326.
124 D. Falconnet, G. Csucs, H. M. Gradin and M. Textor, *Biomaterials*, 2006, **27**, 3044–3063.
125 A. Khademhosseini, R. Langer, J. Borenstein and J. P. Vacanti, *Proc. Natl. Acad. Sci. U. S. A.*, 2006, **103**, 2480–2487.
126 W. F. Liu and C. S. Chen, *Mater. Today*, 2005, **8**, 28–35.
127 C. S. Chen, X. Jiang and G. M. Whitesides, *MRS Bull.*, 2005, **30**, 194–201.
128 T. Xu, J. Jin, C. Gregory, J. J. Hickman and T. Boland, *Biomaterials*, 2005, **26**, 93–99.
129 A. S. G. Curtis, *Eur. Cells Mater.*, 2004, **8**, 27–36.
130 T. H. Park and M. L. Shuler, *Biotechnol. Prog.*, 2003, **19**, 243–253.
131 D. R. Jung, R. Kapur, T. Adams, K. A. Giuliano, M. Mrksich, H. G. Craighead and D. L. Taylor, *Crit. Rev. Biotechnol.*, 2001, **21**, 111–154.
132 A. Folch and M. Toner, *Annu. Rev. Biomed. Eng.*, 2000, **2**, 227–256.
133 C. S. Chen, M. Mrksich, S. Huang, G. M. Whitesides and D. E. Ingber, *Science*, 1997, **276**, 1425–1428.
134 C. H. Thomas, J. H. Collier, C. S. Sfeir and K. E. Healy, *Proc. Natl. Acad. Sci. U. S. A.*, 2002, **99**, 1972–1977.
135 R. McBeath, D. M. Pirone, C. M. Nelson, K. Bhadriraju and C. S. Chen, *Dev. Biol.*, 2004, **6**, 483–495.
136 C. M. Nelson, R. P. Jean, J. L. Tan, W. F. Liu, N. J. Sniadecki, A. A. Spector and C. S. Chen, *Proc. Natl. Acad. Sci. U. S. A.*, 2005, **102**, 11594–11599.
137 S. N. Bhatia, U. M. L. Yarmush and M. Toner, *J. Biomed. Mater. Res.*, 1997, **34**, 189–199.
138 M. Yamato, C. Konno, M. Utsumi, A. Kikuchi and T. Okano, *Biomaterials*, 2002, **23**, 561–567.
139 A. Khademhosseini, K. Y. Suh, J. M. Yang, G. Eng, J. Yeh, S. Levenberg and R. Langer, *Biomaterials*, 2004, **25**, 3583–3359.
140 D. T. Chiu, N. L. Jeon, S. Huang, R. S. Kane, C. J. Wargo, I. S. Choi, D. E. Ingber and G. M. Whitesides, *Proc. Natl. Acad. Sci. U. S. A.*, 2000, **97**, 2408–2413.
141 M. D. Tang, A. P. Golden and J. Tien, *J. Am. Chem. Soc.*, 2003, **125**, 12988–12989.
142 Y. Ito, G. Chen, Y. Guan and Y. Imansihi, *Langmuir*, 1997, **13**, 2756–2759.
143 J. Nakanishi, Y. Kikuchi, T. Takarada, H. Nakayama, K. Yamaguchi and M. Maeda, *J. Am. Chem. Soc.*, 2004, **126**, 16314–16315.
144 J. Nakanishi, Y. Kikuchi, S. Inoue, K. Yamaguchi, T. Takarada and M. Maeda, *J. Am. Chem. Soc.*, 2007, **129**, 6694–6695.
145 J. Edahiro, K. Sumaru, Y. Tada, K. Ohi, T. Takagi, M. Kameda, T. Shinbo, T. Kanamori and Y. Yoshimi, *Biomacromolecules*, 2005, **6**, 970–974.
146 T. Boontheekul and D. J. Mooney, *Curr. Opin. Biotechnol.*, 2003, **14**, 559–565.
147 R. Vasita and D. S. Katti, *Expert Rev. Med. Devices*, 2006, **3**, 29–47.
148 M. P. Lutolf and J. A. Hubbell, *Nat. Biotechnol.*, 2005, **23**, 47–55.
149 H. J. Kong and D. J. Mooney, *Nat. Rev. Drug Discovery*, 2007, **6**, 455–463.
150 K. Saha, J. F. Pollock, D. V. Schaffer and K. Healy, *Curr. Opin. Chem. Biol.*, 2007, **11**, 381–387.
151 D. Seliktar, *Ann. N. Y. Acad. Sci.*, 2005, **1047**, 386–394.

This journal is © The Royal Society of Chemistry 2008

eXPRESS Polymer Letters Vol.2, No.3 (2008) 165–183
Available online at www.expresspolymlett.com
DOI: 10.3144/expresspolymlett.2008.22

Stimuli-responsive poly(ampholyte)s containing L-histidine residues: synthesis and protonation thermodynamics of methacrylic polymers in the free and in the cross-linked gel forms

M. Casolaro[1], Y. Ito[2,3], T. Ishii[2], S. Bottari[4], F. Samperi[5], R. Mendichi[6]*

[1]Dipartimento di Scienze e Tecnologie Chimiche e dei Biosistemi, Via Aldo Moro 2, Università degli Studi di Siena, I-53100 Siena, Italy
[2]RIKEN (The Institute of Physical and Chemical Research), Hirosawa 2-1, Wako, Saitama 351-0198, Japan
[3]Kanagawa Academy of Science and Technology, KSP East 309, Sakado 3-2-1, Takatsu-ku, Kawasaki, Kanagawa 213-0012, Japan
[4]Dipartimento di Fisica, Via Roma, Università degli Studi di Siena, I-53100 Siena, Italy
[5]Istituto di Chimica e Tecnologia dei Polimeri – Sez. Catania (CNR) – Dipartimento di Chimica, Università di Catania, Viale A. Doria 6, I-95125 Catania, Italy
[6]Istituto per lo Studio delle Macromolecole (CNR), Via E. Bassini 15, I-20133 Milano, Italy

Received 12 November 2007; accepted in revised form 14 January 2008

Abstract. Methacrylate-structured poly(ampholyte)s were synthesized in the homopolymer and copolymer forms starting from the *N*-methacryloyl-L-histidine (MHist) and the *N*-isopropylacrylamide (NIPAAm). They were also obtained in the cross-linked (hydrogel) form, showing a close thermodynamic behaviour as that shown by the corresponding soluble free polymer analogues. Viscometric data revealed that the minimum hydrodynamic volume of the polymer at its isoelectric point (pH 5) shifted to lower pHs as the NIPAAm content increased, and beyond a critical low MHist content the reduced viscosity decreased, even at low pHs. The phenomenon was attributed to hydrophobic forces between the isopropyl groups outweighing the repulsive electrostatic interactions of the polymer in the positively charged form. A similar behaviour was shown by the corresponding hydrogel. The latter also revealed a different phase transition phenomenon induced by external stimuli (temperature, pH, ionic strength, electric current) when compared to the acrylate-structured analogues. The polyMHist, as well as the corresponding monomer, was found for two days to be non toxic against the mouse osteoblasts (MC3T3-E1).

Keywords: *biocompatible polymers, smart polymers, polymer gels, protonation thermodynamics, polyampholytes*

1. Introduction

Vinyl compounds carrying aminoacid residues have been widely synthesized to obtain functional polymers for practical purposes [1]. The presence of the carboxyl [2] or the amino [3] functionality made these polymers sensitive to the pH in a range that was closely related to their basicity constants. Moreover, the presence of the hydrophilic amido functionality and the hydrophobic isopropyl groups in the side chain made these polymers also sensitive to the temperature [4, 5].

Recently, new vinyl acrylate polymers based on the L-histidine residues have been developed in order to have poly(ampholyte)s responding in different pH-ranges [6]. The imidazole-containing methacrylate polymers with different functions were investi-

*Corresponding author, e-mail: casolaro@unisi.it
© BME-PT and GTE

gated in the catalytic activities towards the solvolyses of a series of activated phenyl esters [7]. Besides the buffering capacity of proteins in the physiological pH range, the imidazole group is also able to form coordination compounds with metal ions [8]. These compounds are considered as models for the understanding of the biological activity of proteins involved in fatal disorders such as the Alzheimer's disease or the prion infection [9, 10]. Synthetic polymers containing the imidazole functionality have recently been reported as thermosensitive, reusable displacers for immobilized metal affinity chromatography of proteins [11, 12]. The incorporation of the imidazole functionality in the highly branched poly(*N*-isopropylacrylamide), the polyNIPAAm, showed interest as a thermally responsive 'smart' polymer for the purification of a histidine-tagged protein fragments [13, 14]. Moreover, the absence of toxicity makes these ampholyte polymers useful candidates in the development of loosely cross-linked hydrogels to be used as injectable polymer scaffolds for tissue engineering applications [15]. The non toxic effect of the poly(MHist) against the osteoblast cells enables the corresponding hydrogels to be tailored in medical treatment for more efficient routes in the administration of pharmaceutical compounds, especially metal-based drugs [16], and improves the absorption of loaded amino-bisphosphonates (BPs) in the bone resorption process [17, 18]. In the latter case, the poor absorption of bisphosphonates via the paracellular route may be improved by a slow releasing process of BPs loaded into the hydrogel. Previous reported papers described the thermodynamic behaviour of acrylate polymers with the L-histidine residues in the free and in the cross-linked forms [6]. Copolymers with the *N*-isopropylacrylamide were also prepared to obtain multiple stimuli-sensitive hydrogels for biomedical applications [19, 20]. In fact, besides the pH, they were sensitive to the temperature, the electric potential, the salt-type and the ionic strength.

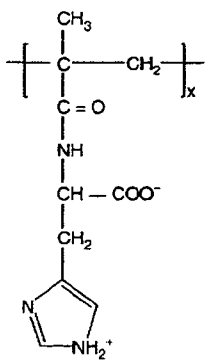

Figure 1. Structure of the monomer unit of poly(MHist)

Following our interest in these kind of polymers, we thought to study the methacrylate-structured polymer analogues because, as a rule, the solution behaviour of acrylate compounds differs to some extent from that of the corresponding methacrylate [21]. Thus, the aim of this paper is devoted to the protonation behaviour study of the synthetic methacrylic poly(ampholyte)s containing the L-histidine residues, the poly(MHist) (Figure 1).

A series of copolymers with a variable amount of NIPAAm was studied in order to clarify their thermodynamic behaviour in view of the potential applications of the corresponding hydrogels. The thermodynamic study of either the soluble or the cross-linked polymers allowed to evaluate the basicity constants along with the enthalpy and entropy changes during the protonation of the imidazole nitrogen. Moreover, the results of the swelling properties of three different cross-linked hydrogels were reported along with their protonation behaviour. They were strictly compared to the previously reported acrylate analogues [6, 19].

The hydrophilic behaviour of the non toxic poly (MHist) allowed the preparation of a new type of copolymer for nonbiofouling surfaces [22]. The polystyrene hydrophilization with poly(MHist) and some of its copolymers was in fact shown to be higher than that of the BSA (Bovine Serum Albumin).

2. Experimental section

2.1. Materials

L-Histidine (98%), methacryloyl chloride (97%) and 2,2'-azoisobutironitrile (AIBN, 98%) were purchased from Wako Pure Chemical Industries. Ammonium peroxo-disulfate (APS, 98%) and *N,N,N',N'*-tetramethylethylenediamine (TEMED) were from Kanto Chemical *Co.*, Inc. *N,N'*-ethylenebis-acrylamide (EBA, 98%) and triethylamine (TEA, 99.5%) were from Fluka *Co.* The AIBN was recrystallized from methanol and all the other reagents were used as received. The *N*-isopropylacrylamide (NIPAAm, Wako Co.) was purified by recrystallization from *n*-hexane and then dried in vacuo. Buffer solutions (tris, phosphate, acetate)

were prepared at a concentration of 0.01M in twice-distilled water and in 0.15M NaCl. The sodium chloride salt was of analytical grade from Fluka *Co.*

2.2. Syntheses

Synthesis of MHist

The *N*-methacryloyl-L-histidine, MHist, was prepared according to the previously reported synthetic routes [22, 24]. To an aqueous solution of L-histidine (5.0 g, 32 mmol) and sodium hydroxide (1.6 g, 40 mmol) in twice-distilled water (20 ml), the methacryloyl chloride (3.67 ml, 38 mmol), diluted in dioxane (10 ml), was added dropwise. During addition, the reaction mixture was kept under 5°C by the external ice-bath cooling, and then the temperature was raised to room temperature for 1 hour. After removing the dioxane by a rotary evaporator, the mixture was acidified to pH 2 with concentrated hydrochloric acid and extracted with ether. The aqueous layer was adjusted to pH 5 and concentrated in vacuo to obtain crude MHist. The crude monomer was purified by repeated precipitations from ethanol to acetone and dried in vacuo.

Synthesis of polyMHist

The poly(*N*-methacryloyl-L-histidine), polyMHist, was synthesized by a conventional free-radical polymerization [25]. The polymer was obtained as follows. A mixture of MHist (0.5 mmol) in ethanol (20 ml) containing AIBN (0.05 mmol) was purged with N_2 gas and then allowed to react under nitrogen atmosphere at 70°C for 20 h. The obtained polymer was purified by using a dialysis cellophane tubing-seamless (MWCO 3500 g/mol) in twice-distilled water for 2 days and then lyophilized to give a white powder.

Synthesis of poly(MHist-co-NIPAAm)

The poly(*N*-methacryloyl-L-histidine-*co*-*N*-isopropylacrylamide), poly(MHist-*co*-NIPAAm), copolymers were synthesized by the conventional free-radical polymerization reaction. Three different samples of the NIPAAm/MHist copolymers with decreasing amounts of MHist, namely co-3, co-2, and co-1, were synthesized. The mixture of MHist and NIPAAm with different molar ratio (the total mole was adjusted to 20 mmol) in twice-distilled water (40 ml), and containing 30 µl of TEMED 10 mM solution, was purged with N_2 gas and then 100 µl of APS 5 mM solution were added and allowed to react under nitrogen atmosphere at room temperature for 18 h. The polymer obtained was purified by using a dialysis cellophane tubing-seamless (MWCO 3500 g/mol) in twice-distilled water for 2 days and then lyophilized to give a white powder.

Synthesis of hydrogels

Three hydrogel samples containing only MHist (MH2) and a mixture of NIPAAm/MHist (CMH2, CMH10), were prepared according to a previously reported procedure [6, 19, 26]. The two poly (MHist-*co*-NIPAAm) hydrogels, at a NIPAAm/MHist molar ratio of 12, were synthesized by cross-linking with 2 (CMH2) and 10 (CMH10) mol% of EBA. The hydrogel MH2 was obtained only with the MHist cross-linked with 2 mol% of EBA. The synthesis was carried out in a glass tube, containing the monomer solution at a total concentration of 15 wt%, after their degassing under vacuum and under a nitrogen atmosphere. The reaction mixture was kept at room temperature for 24 h even if the gelation was observed within 4 h. Afterwards, the gel samples were removed, thoroughly washed with twice-distilled water for two weeks, and then slowly dried at r.t. to a constant weight. In all cases, the yield was more than 90%.

2.3. Spectroscopic and molecular characterization

The molecular characterization of polyMHist homopolymer and related copolymers was performed by a multi-angle laser light scattering (MALS) Dawn DSP-F photometer from Wyatt (Santa Barbara, CA, USA) on-line to a size exclusion chromatography (SEC) system. The SEC-MALS experimental conditions were the following: 0.2M NaCl + 0.1M Tris buffer pH 8.0 as mobile phase, two TSKgel PW G4000 and G3000 columns from Tosoh Bioscience (Stuttgart, D), 35°C of temperature, 0.8 ml/min of flow rate and 150 µl of injection volume. The wavelength of the MALS He-Ne laser was 632.8 nm. The light scattering signal was simultaneously detected at fifteen

scattering angles ranging in the solvent from 14.5° to 151.3°. The calibration constant was calculated using toluene as standard assuming a Rayleigh Factor of $1.406 \cdot 10^{-5}$ cm^{-1}. The angular normalization was performed by measuring the scattering intensity of a concentrated solution of a BSA globular protein in the mobile phase assumed to act as an isotropic scatterer. The refractive index increment, dn/dc, of polyMHist homopolymer and copolymers with respect to the used solvent was measured by a KMX-16 differential refractometer from LDC Milton Roy (Riviera Beach, FL, USA). The dn/dc values were: polyMHist: 0.190 ml/g, co-1: 0.175 ml/g, co-2: 0.177 ml/g, co-3: 0.182 ml/g. Proton NMR spectra of the monomer and the polymers were recorded in D_2O on a 400 MHz spectrometer (JEOL EX400, Japan). The FT-infrared spectra of the same compounds were recorded on a FTS 6000 Biorad spectrophotometer. The MALDI-TOF mass spectra were recorded in the reflection mode, using a Voyager-DE STR instrument (Perseptive Biosystem) mass spectrometer, equipped with a nitrogen laser (λ = 337 nm, pulse width = 3 ns), working in a positive ion mode. The accelerating voltage was 25 kV, the grid voltage and the delay time (delayed extraction, time lag) were optimized for each sample to achieve the higher mass resolution (FWHM). The laser irradiance was maintained slightly above threshold. The samples used for the MALDI analyses were prepared as follows: 10 µl of polymer solution (10 mg/ml in H_2O or C_2H_5OH) were mixed with 30 µl of HABA solution (0.1M in C_2H_5OH), then 1 µl of each analyte/matrix mixture was spotted on the MALDI sample holder and slowly dried to allow the analyte/matrix co-crystallization. A mass resolution of about 4000 Da was obtained in the best MALDI mass spectra recorded.

2.4. Viscometric measurements

Viscometric measurements were carried out with an AVS 310 automatic Schott-Gerate viscometer at 25°C on a dilute aqueous polymer solution. The solution was freshly prepared by weighing and dissolving a known amount of the polymeric compound (MHist content, mmol: polyMHist, 0.2154; co-3, 0.2258; co-2, 0.2258; co-1, 0.1368) in 25 ml of 0.15M NaCl containing a measured volume of standard 0.1M NaOH solution. A standard 0.1M HCl solution was stepwise delivered by a Metrohm Multidosimat piston buret. The evaluation of the pH, at each neutralization step, was made with the program Fith [27] from the $\log K^{\circ}$ and the n values of the corresponding polymer and copolymers (see basicity constants, section 3.2). Viscometric data at different temperatures were obtained on polymer solutions at three different significant pHs (9, 5, and 2). A weighed amount of copolymer (co-1, 336 mg; co-2, 282 mg; co-3, 97.9 mg) was dissolved in 25 ml of 0.15M NaCl and the pH was controlled by adding the stoichiometric quantity of standard NaOH or HCl solutions. The temperature was monitored by the Haake DC10 thermostat (Thermo Electr. Corp.).

2.5. Potentiometric measurements

The acid-base potentiometric measurements were carried out in aqueous media at 25°C, following a previously reported procedure [6, 19]. A TitraLab 90 titration system (from Radiometer Analytical), consisting of three components (Titration Manager, TIM900; high-precision autoburet, ABU901; and the sample stand) and connected to the TimTalk 9 (a Windows based software, for remote control) was used to record the potentiometric titration data of the monomer, the polymers, and the hydrogel. All the titrations were carried out in a thermostated glass cell filled with 100 ml of 0.15M NaCl in which a weighed quantity of solid material and a measured volume of standard HCl solution were dispersed by magnetic stirring, under a presaturated nitrogen stream. Forward titrations were carried out with a standard 0.1M NaOH solution and reliable results were obtained for the back-titration with a standard 0.1M HCl solution. Unlike the monomer and the polymers, which, being soluble over the whole pH-range investigated were titrated at the equilibration time of 300 s for each titration step (0.04 ml), the MH2 roughly and finely crushed hydrogel sample (0.1205 mmol) was titrated at different equilibration times (1500 and 3000 s). In the case of the roughly crushed hydrogel, hysteresis loops were obtained during the forward and backward titrations with NaOH and HCl standard solutions, respectively; the finely crushed hydrogel improved a faster response in reaching equilibrium conditions. A typical potentiometric titration curve for the soluble compounds is reported in Figure 2,

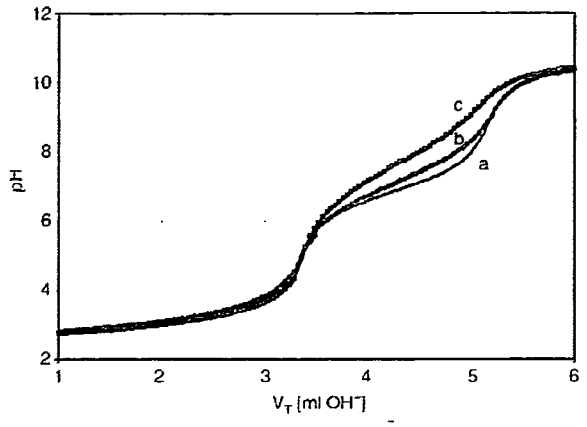

Figure 2. Potentiometric titration curves (pH in relation to the volume of standard NaOH 0.1084M) of MHist (a, 0.1997 mmol), co-3 (b, 0.2090 mmol), and polyMHist (c, 0.1864 mmol) in 0.15M NaCl at 25°C

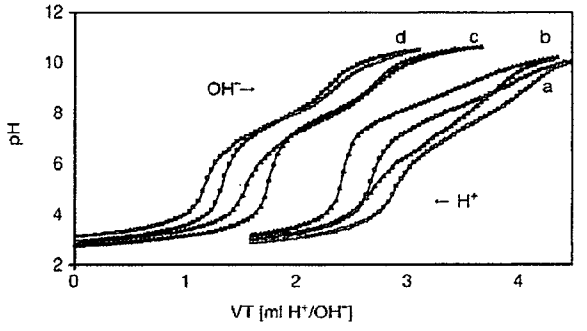

Figure 3. Potentiometric titration curves of the MH2 hydrogel (a, b: roughly crushed; c, d: finely crushed) protonation in 0.15M NaCl at 25°C. Equilibration time for each titrant addition (0.04 ml of 0.1205M NaOH forward, blue curves; 0.04 ml 0.1123M HCl backward, red curves): 1500 s (triangle) and 3000 s (square)

while Figure 3 shows the titration curves of the MH2 hydrogel in the rough and fine crushing state. The basicity constant (log*K*) values of the monomer were evaluated with the Superquad program [28] taking into account all the points of three independent potentiometric titration curves (ca. 300 data points) carried out with a different amount of ligand (0.13–0.20 mmol). On the other hand, the basicity constants of the free (polyMHist, 0.15–0.19 mmol; co-3, 0.21 mmol; co-2, 0.23 mmol; co-1, 0.13 mmol) and the cross-linked polymers (MH2, 0.12–0.15 mmol) were evaluated with the ApparK program [27]. In these cases each potentiometric titration was computed to evaluate both the log*K*s into a separated pH-buffered region. In all cases, the $E°$ calibrations were performed before and after each titration with the standard Tris grade-reagent. Three replicates were averaged and their standard deviations calculated.

2.6. Calorimetric measurements

Calorimetric measurements were carried out in aqueous solution at 25°C, following a previously reported procedure [6], by the use of a Tronac titration calorimeter (mod 1250) operating in the isothermal mode. A stainless steel reaction vessel was filled with 25 ml of 0.15M NaCl (containing a measured amount of standard NaOH solution) in which a weighed quantity of solid material (MHist content, mmol: monomer MHist, 0.12–0.24; polyMHist, 0.14–0.22; co-3, 0.13–0.23; co-2, 0.13–0.23; co-1, 0.14) was dissolved and titrated with a standard 0.1M hydrochloric acid solution at a BDR (buret delivery rate) of 0.0837 ml/min through a Gilmont buret. The titrations were performed at high and low MHist content for the protonation of the only imidazole nitrogen and for the protonation of both the imidazole and the carboxylate groups, respectively. Before and after each experiment, the chemical calibration with Tris/HCl and the corrections for the heats of the titrant dilution were made. All the experiments were automatically controlled by the Thermal program (from Tronac, Inc.) which was renewed to operate through a NI-DAQ driver software in Windows (from National Instruments). The graphical programming language LabVIEW was used to create the application. The evaluation of the enthalpy change ($-\Delta H°$) values was obtained with the Fith program [27] by taking into account the linear dependence of the log*K*s on α (the degree of protonation) for the polymeric compounds. The entropy change ($\Delta S°$) values were calculated. The results of at least two replicates were averaged.

2.7. Swelling measurements

Swelling measurements of the hydrogels (MH2 and CMH2) were carried out in different conditions of pH and temperature, at equilibrium conditions. The equilibrium degree of swelling (EDS) was measured every 24 h because the kinetic DS/time curves reached a plateau in these conditions. A weighed sample of dry gel (MH2, 30.4 mg; CMH2, 28.7 mg), contained in a Strainer cell (100 μm pore size), was immersed in a thermostated glass cell filled with

100 ml of aqueous solution at the desired pH, under stirring by the magnetic bar. The temperature probe and the pH glass electrode were controlled by the TimTalk 9 software. The EDS in relation to pH for both the hydrogels was monitored at different pHs of the proper buffer. The EDS in relation to the sodium chloride concentration was monitored at 25°C and in Tris/HCl buffered solution at pH 9.02 by the daily addition of weighed portions of the salt to produce the desired final concentration. The effect of the temperature for the CMH2 gel was monitored in buffered solutions at three different pHs (9.02, 5.01, and 3.07) and at a constant ionic strength (0.15M NaCl). In all cases, the gel sample and its container were removed from the bath at intervals, blotted with a tissue paper to remove any surface droplets, and weighed (wet weight, W_{wet}). The procedure was repeated at 12–24 h intervals. The EDS value was calculated by the relation: $EDS = (W_{wet}-W_{dry})/W_{dry}$, where W_{dry} is the weight of the dry gel sample.

2.8. Electric measurements

Hydrogels contraction measurements were carried out at 25°C according to the previously reported procedure [19]. A constant voltage was applied between two gold electrodes (16 mm diameter) in a cylindrical nylon cell, and with a mobile cathode positioned on the gel sample. The hydrogels (CMH2 and CMH10) were swollen in a 0.01M Tris/HCl buffer solution at pH 9, then a specimen of 5 mm thick was cut and used for contractile experiments for a period of 10 min. Under the application of the electric field, each hydrogel change in the thickness was controlled by a digital comparator that was sensitive to displacements of 10^{-2} mm (Digimatic indicator 266-2745, Mitutoyo). All the experiments were controlled through a NI-DAQ driver software in Windows (from National Instruments) and the graphical programming language LabView was used to create the application. The gel deformation was recorded at intervals of 1 s under the applied voltage (2.5, 5.0, and 7.0 V) by a dc power supply.

2.9. Evaluation of cytotoxicity

Cell culture

Mouse osteoblast cells (MC3T3-E1) obtained from the RIKEN Cell Bank (Tsukuba, Ibaraki, Japan) were cultured to confluence in culture dishes (Corning *Co., Ltd.*) containing a medium composed of Minimum Essential Medium, alpha modified (MEM-α, Kohjin Bio *Co. Ltd.*, Japan) supplemented with 10% fetal bovine serum (FBS,BioWest, France) in a fully humidified atmosphere with a volume fraction of 5% CO_2 at 37°C.

Cytotoxicity evaluation

The cell viability was evaluated by using a Cell Counting Kit [29] (WST-1 method, Dojindo Lab., Tokyo, Japan). Briefly, after the MC3T3-E1 cells reached confluency, they were trypsinized and seeded at $1 \cdot 10^4$ cells/cm^2 onto 96-well multiplate (Corning *Co., Ltd.*) then incubated for 2 days in a humidified atmosphere containing 5% CO_2 at 37°C. After removing the cultured medium, 100 µl of fresh culture medium supplemented with 10% [v/v] FBS and containing each MHist sample were added to each well and allowed to stand for in a fully humidified atmosphere with a volume fraction of 5% CO_2 at 37°C. After 24 h of incubation, 10 µl of WST-1 reagent were added to each well and the wells incubated for 2 h at 37°C; then 10 µl of 0.1N HCl aqueous solution were added to each well to stop the reaction. The absorbance of aliquot of the solution was measured at 450 nm, with a reference of the absorbance at 655 nm, with a multiplate reader (Bio-Rad model 650, Tokyo, Japan). The results were expressed as viability [%] related to a control containing no MHist samples. The error bar means standard error of four experiments.

3. Results and discussion

3.1. Syntheses and characterization

Monomer

The *N*-methacryloyl-L-histidine (MHist) was prepared according to the synthetic route to obtain vinyl monomers from α-aminoacids [2, 4–6, 22–24]. The reaction between methacryloyl chloride and L-histidine at low temperature (< 5°C) allowed to obtain a white powder freely soluble in water. The